Chapter 5:

Assaying Bridge Occupation in DNA-mediated Electrochemistry

5.1: INTRODUCTION

It has been proposed that DNA-mediated charge transport (CT) can be considered in two separate regimes.[1] In the first regime, charge that is injected at higher energy than the DNA bridge propagates by hopping between nucleotides. This process involves real occupation of the DNA. When the hole (electron) donor has inadequate potential to oxidize (reduce) the HOMO (LUMO) of the individual base pairs, then the bridge is only virtually occupied, and superexchange, with its consequently strong distance dependence, is the mechanism of CT. While there is now ample evidence that both types of CT occur in DNA,[2] this neat division based on the energy of the donor is not consistent with much of the existing evidence. Examples include the DNA-mediated long-range quenching of photoexcited Ru(II) or ethidium bromide intercalators by $[Rh(phi)_2(phen')]^{3+}$, and the transport of charge between stilbenes through a higher energy adenine tract.[3-5]

Over the previous decade, the Barton group has demonstrated that ground-state DNA-mediated CT can be achieved over long distances, with minimal loss of yield, in the context of DNA self-assembled monolayers on electrodes.[6] These systems are energetically analogous to DNA-mediated CT between proteins, which plays an essential role in lesion detection, and possibly other biological roles.[7] The DNA-mediated nature of this reaction has been demonstrated by the dependence of the yield and rate on structural parameters. CT rate decreases as the length of the alkyl surface linker increases, with a β of 1 $Å^{-1}$, indicating that CT is mediated by the covalent linker to the DNA.[8] Furthermore, probes designed to feature poor electronic conjugation to the DNA π-stack also show impaired CT yield.[9,10] Finally, as in other systems, structurally minimal perturbations that disrupt the DNA π-stack also attenuate DNA-mediated electrochemistry.[11-13] Importantly, if the electrochemical probes were instead dynamically

accessing the surface,[14] each of these conditions would have the *opposite* effect on CT rate and yield to that which is observed.

To summarize, three properties of DNA-mediated electrochemistry are particularly counter-intuitive with respect to theory.[6] First, probes are observed near their free potentials, covering a range of nearly a volt.[15] Second, DNA reduction has not been observed in this range in the absence of a probe. Third, none of the DNA bases are energetically within, or even near, the voltammetric range of electrochemical probes that have been applied.[16] These three properties are all inconsistent with direct oxidation of the DNA.

The incompatibility of the last property with a hopping mechanism can be demonstrated by considering the expected rate of charge injection. As demonstrated in Chapter 1, using extremely favorable parameters, the rate of injection from the electrode to an iron-sulfur cluster (0.1 V vs. NHE) is necessarily far below that of 0.002 s^{-1}. This is slower than the observed linker-limited rate of 30 s^{-1}, implying that hopping is not a reasonable mechanism for DNA-mediated electrochemistry due to the slow thermal population of the bridge.

However, in the absence of hopping, it is hard to explain the insensitivity of DNA-mediated electrochemistry to the length of the DNA.[11] The CT rate continues to be limited by tunneling through the linker even for a DNA bridge length of 11 nm.[17] For a modest β of 0.2 $Å^{-1}$,[18] the frequency factor would have to be a respectable 1 x 10^{11} s^{-1} to be consistent with experiment; however, this far from the bridge energies, β is by necessity much higher. Using the expression:

$$\beta = \frac{2}{a}\ln\left[\frac{\Delta\varepsilon}{2V} + \sqrt{1+\frac{\Delta\varepsilon^2}{4V^2}}\right] \qquad \textbf{(5.1)}$$

with a typical interbase coupling V of 0.05 V,[19] the energy gap $\Delta\varepsilon$ as 1 V, and a, the intersite separation as 3.4 Å yields a β of 1.8 Å^{-1}. For this β, a preexponential factor of 10^{87} s^{-1} is necessary to explain the experiment. This is unreasonable. Hence, for superexchange to be the dominant mechanism of DNA-mediated electrochemistry, very low β is necessary despite the distance between the donor and acceptor energies and the energy of the bridge states.

Although hopping and superexchange both seem unreasonable, there is no other mechanism that has been proposed for CT. To elucidate the nature of DNA-mediated electrochemistry, we consider the essential question of whether the DNA is, in fact, occupied and what the nature of these occupied intermediates might be. To answer this question, we perform electrochemistry on DNA containing a fast radical trap, analogous to those used in Chapters 2 and 3.

The *N*-cyclopropyl charge reporter has been used to demonstrate occupation of guanine, adenine and cytosine during DNA-mediated CT in solution. Particularly, N_4-cyclopropylcytosine (^{CP}C) is a fast reporter for DNA reduction.[20,21] This reporter can reveal analogous information about DNA-mediated electrochemistry. Herein, we develop and apply an assay for this chemical reaction in DNA films.

5.2. METHODS

5.2.1. DNA SYNTHESIS AND PREPARATION

DNA oligonucleotides were synthesized trityl-on using standard phosphoramidite chemistry on an ABI DNA synthesizer with Glen Research reagents. Redmond Red was incorporated on the 3' terminus by extension of the oligonucleotide on Redmond Red-labeled beads (Glen Research), using UltraMILD reagents (Pac-dG, iPr-Pac-dA, Ac-dC,

and phenylacetic anhydride capping mix (Glen Research). These strands were ultimately deprotected and cleaved from the resin by shaking the beads in 50 mM K_2CO_3 in dry methanol for several hours, then shaking in fresh solution for several hours. The aliquots of base solution were combined and lyophilized. ^{CP}C-modified oligonucleotides were prepared by incorporating the precursor base, 4-cyanoethylthio-uridine (Glen Research) as a phosphoramidite at the desired position, followed by deprotection of the cyanoethyl with 1 M DBU in dry acetonitrile for three hours. The oligonucleotides were subsequently incubated overnight in 6 M aqueous cyclopropylamine (Aldrich) at 60 ^{o}C. resulting in substitution, base deprotection, and simultaneous cleavage from the resin. The cleaved strands were dried *in vacuo* and purified by reversed-phase HPLC, detritylated by 80% acetic acid for 15 min, and repurified by reversed-phase HPLC. Oligonucleotides were characterized by MALDI-TOF mass spectrometry and UV-vis spectrophotometry.

For oligonucleotides containing a thiol linker, the strands were prepared without the terminal DMT group, and the linker added as previously described.[11] All duplex DNA was of the sequence:

CP-dsDNA: 5'- CGCGATGA^{CP}CTGTACT-3'

3'-RR-GCGCTACT GACATGA- OC(O)NH$(CH_2)_6$NHC(O)$(CH_2)_2$-5'-SH

where RR represents the Redmond Red. DNA was also prepared without the CP-modification, for use as a standard corresponding to the oxidation decomposition product.[22,23] Purified oligonucleotides were annealed together in degassed buffer at 100 μM, by heating to 90 ^{o}C for 5 minutes and slowly cooling to ambient temperature

over 90 minutes. Phosphate buffer (PB: 5 mM P_i, 50mM Na, pH 7.0) was used for all experiments.

5.2.2. Film Preparation and Electrochemistry

To assemble films, Au(111) surfaces on mica on glass, stored under N_2, were used (GE Healthcare). Upon removal from inert atmosphere, surfaces were immediately inserted into a cell, with a 7 mm diameter o-ring in direct contact with the surface. Into this cavity, 50 μM DNA, 100 mM $MgCl_2$ in PB was pipetted. Cells were stored under high humidity, in the dark, and at 4 ^oC for 20 to 50 hours. The solution was removed and saved for reuse, on the condition that HPLC analysis confirms its stability. All thiolated DNA was stored degassed and frozen, under Ar. Surfaces were washed with PB, 1 mM mercaptohexanol in 1% ethanol and PB was added, and the surface stored in the above conditions for 60 - 90 minutes. Surfaces were well washed, and then subjected to electrochemical assay with three-electrode configuration using a Ag/AgCl/(4% agarose in 3 M NaCl) reference electrode and Pt counterelectrode in a Faraday cage. Cyclic voltammetry (CV) (v = 100 mV/s) and chronocoulometry (CC) experiments were performed at ambient temperature on an electrochemical analyzer (CH Instruments, Austin, TX).

5.2.3. DNA Recovery and Analysis

A variety of recovery methods were attempted, with the best success achieved with mild heating of the gold surface to 70 ^oC, successive washes with PB at that temperature, fast cooling to 4 ^oC, immediate cold filtration (0.2 μm) of the collected washes, and immediate analysis by HPLC. HPLC was performed on a reversed-phase

analytical C18 column, with a 0.5 %/min gradient from 50 mM NH_4OAc to acetonitrile over the region of interest. The temperature of the buffers was controlled (55 ^oC) over the course of runs. High temperature was used to ensure dehybridization of double-stranded DNA should any be recovered from the film. For every set of experiments, standards for ^{CP}DNA, unmodified DNA, and deposition solution (i.e., double stranded, thiolated, DNA that was used to generate the monolayers) were also analyzed, as was a mercaptohexanol film assembled in the absence of DNA. Unless otherwise noted, all traces are at 260 nm, with the mercaptohexanol film subtracted to minimize background. Standards of the ^{CP}C-containing strand were consecutively run to provide calibration for quantification, although anomalously large peaks were occasionally observed. Quantification was not reliable below 2 pmol (5 pmol/cm^2). Online UV allows discrimination between DNA peaks and peaks due to other compounds.

5.3. RESULTS

5.3.1. HPLC ANALYSIS OF DNA RECOVERED FROM SELF-ASSEMBLED MONOLAYERS

DNA-modified films were generated on gold electrodes by self-assembly driven by covalent thiol on gold association. The DNA contains both the redox label Redmond Red,[17] to establish DNA-mediated CT, and the intervening fast radical trap ^{CP}C. By recovering the DNA after electrochemistry, and analyzing for ^{CP}C decomposition, we can determine some limits on the extent of charge occupation of the bridge. This experimental approach is illustrated in **Figure 5.1**.

The HPLC profile of the recovery solution from mercaptohexanol/Au monolayers shows four main features (**Figure 5.2**). These features were consistent across all films, prepared over many months. Feature A is the solvent front. Feature B is a small peak,

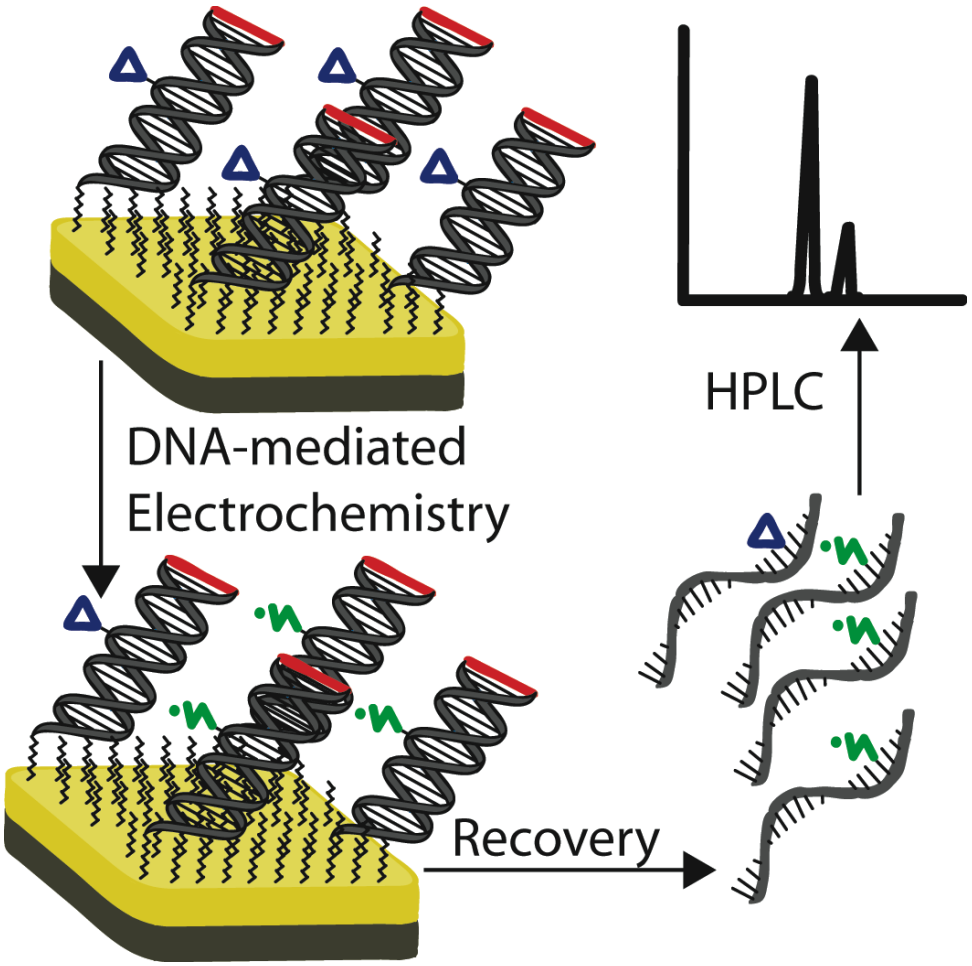

Figure 5.1. Experimental strategy for detecting ^{CP}C ring-opening during DNA-mediated electrochemistry. N_4-cyclopropylcytidine (^{CP}C, blue)- and Redmond Red (RR, red)-containing oligonucleotides were incorporated into a DNA-self assembled monolayer on gold, via the covalent gold-thiol bond. These films were backfilled with mercaptohexanol and subjected to electrochemical analysis. To determine whether this induced ring-opening (green), the relative amount of oligonucleotides containing the decomposition product cytosine and those containing ^{CP}C was quantified by HPLC.

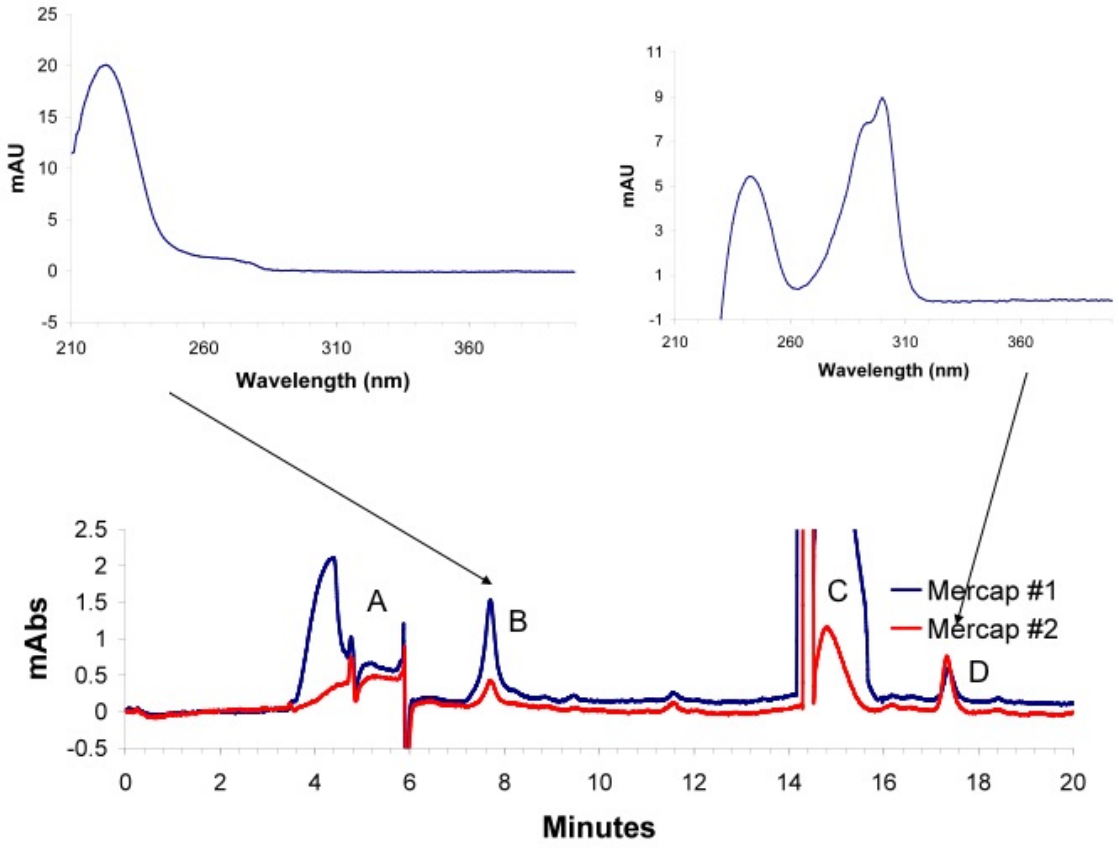

Figure 5.2. HPLC chromatogram (260 nm) of sample prepared by the recovery protocol from a mercaptohexanol self-assembled monolayer on gold. There are four main artifacts, none of which are DNA, observed in aliquots collected from the recovery protocol, as performed on mercaptohexanol films. The earliest (A) peak represents the injection front. The size of the largest (C) is strongly related to the time between recovery and analysis. The left inset indicates the UV-vis spectrum collected online for the pre-DNA elution peak (B), while the right inset is the UV-vis absorption spectrum for a late-eluting peak (D).

earlier than the DNA elution region, with a peak maximum below 220 nm. Feature C is centered far after the DNA elution region. This species absorbs across all wavelengths, indicating that the composition is most likely small particles. The size of this peak can vary from not present at all, to so large as to elute over ten minutes, obscuring the entire profile. This peak was found to depend on the recovery protocol; the cold filtration protocol described above suppresses this peak to negligible levels. Feature D is the latest eluting peak, far from the DNA elution region, and with absorbance maxima at 245 nm and 305 nm. None of these species was produced in adequate yield for mass spectrometric or chemical characterization.

If the recovery protocol is performed on a DNA-S/Au self-assembled monolayer that has been backfilled with mercaptohexanol below 1 mM, or for less than 1 hr, two new peaks appear, both with absorption profiles consistent with being oligonucleotides (data not shown). The first peak corresponds to the complementary (non-thiolated) strand. This assignment was confirmed by co-elution and mass spectrometry. The second peak is faster-eluting, and co-elutes with an impurity that appears in aliquots of the thiolated strand upon oxygen exposure, suggesting it is the sulfate product of the thiolated strand. This was confirmed by mass spectrometry.

To eliminate the sulfate peak, backfilling was extended to 1 hr, with 1 mM mercaptohexanol. This procedure was always successful, over several dozen experiments. One possibility is that more modest backfilling conditions were not successful in removing DNA that was loosely associated with the film.[24] Alternatively, the sulfate-nucleotide could represent a population that is in a different chemical or morphological environment. The former interpretation is consistent with recent work that demonstrates

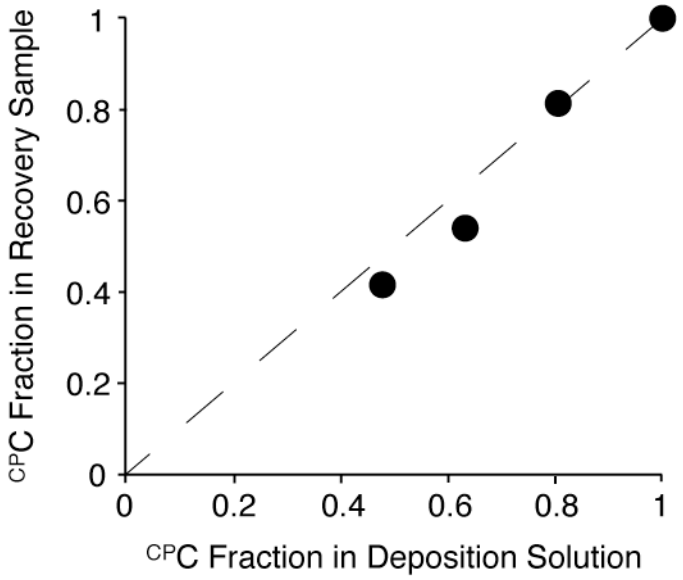

Figure 5.3. Analysis of ^{CP}C content in samples recovered from mixed monolayers. The fraction of ^{CP}C containing DNA, versus DNA containing the ring-opening product cytidine, in the recovery solution is similar to that in the deposition sample. There is little concentration, if any, of ring-opened product in the absence of electrochemical interrogation. The dashed line is unity, and traces at 290 nm were used for these samples.

ready association of non-covalently attached DNA with covalent DNA self-assembled monolayers on gold.

To further validate this technique mixed monolayers were assembled with varying fractions of ^{CP}C-containing and unmodified strands of the same sequence. The relative quantities of ^{CP}C-containing and unmodified strands can be determined by the peak areas by HPLC, as the strands are resolved by over a minute. The relative peak heights were strongly correlated with the monolayer composition (**Figure 5.3**), indicating that the recovery protocol neither induces ^{CP}C decomposition nor selectively enriches one type of oligonucleotide.

5.3.2. HPLC ANALYSIS OF ^{CP}C-DNA AFTER ELECTROCHEMISTRY

Having validated our protocol for recovery and HPLC analysis of ^{CP}C-containing DNA, we explored whether DNA-mediated electrochemistry could induce the ring-opening decomposition of ^{CP}C. Cyclic voltammagrams from electrochemistry on ^{CP}C-containing DNA monolayers did not reveal any novel features. Furthermore, applying cyclic voltammetry did not appear to affect the recovery profile from DNA monolayers.

Since single short pulses were inadequate to induce ring-opening, we explored the effects of both many short pulses and a few long pulses. Four separate films were subjected to pulse sequences of N * (0.5 s, + 60 mV; 0.5 s, -110 mV) for N = 500, 1000, 2000, 4000. Under these conditions, cyclic voltammetry before and after the pulse sequences reveals no loss of the faradaic signal associated with Redmond Red, implying that the film integrity has not been compromised (**Figures 5.4, 5.5** and **Table 5.1**). Furthermore, there is no obvious change in the chromatograms with more pulses.

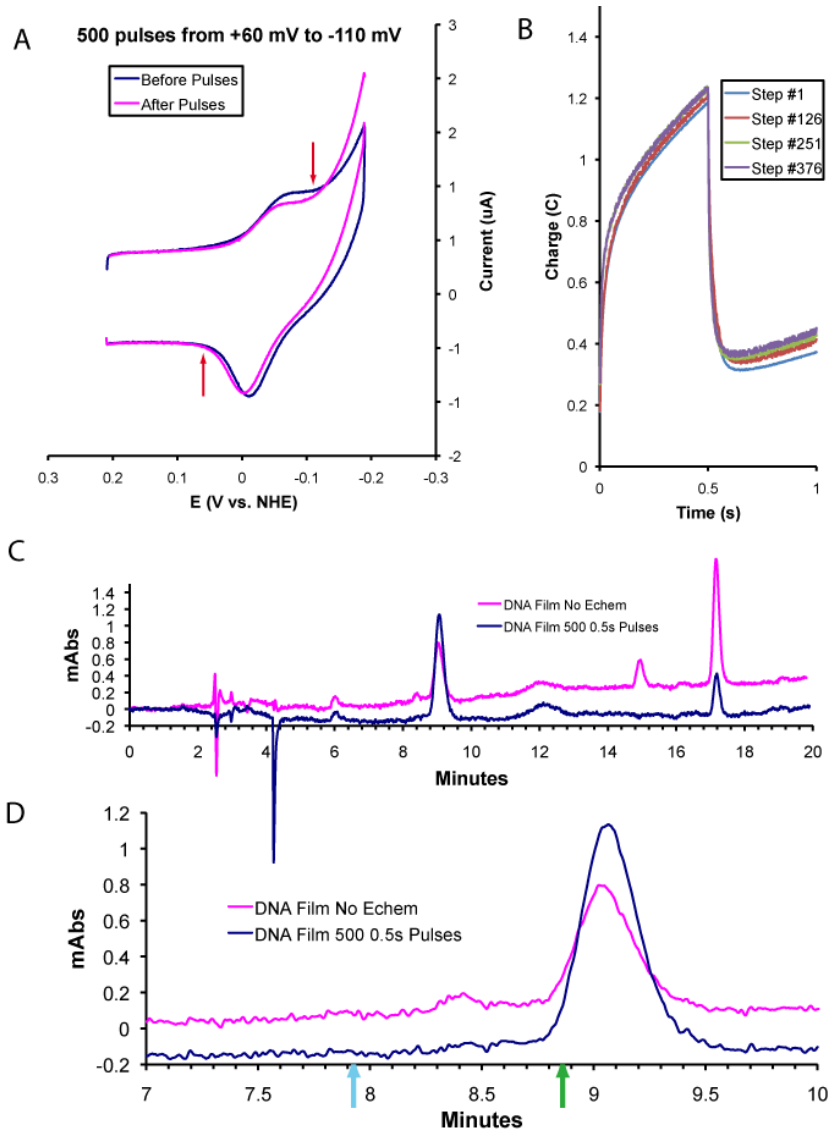

Figure 5.4. Analysis of ^{CP}C content after the pulse sequence 500 x (0.5 s, + 60 mV; 0.5 s, -110 mV). CV before and after the pulse sequence 500 x (0.5 s, + 60 mV; 0.5 s, -110 mV) (A) shows minimal effect of the pulse sequence on the film. Red arrows indicate the potentials switched between for this pulse sequence. Similarly, the CC traces (B) associated with the pulses do show significant change over the course of the pulse sequence. No new peaks are observed in the DNA elution region of the HPLC chromatogram (260 nm) (C, D). The elution times of the standards for DNA with (green arrow) and without (cyan arrow) the ^{CP}C modification are indicated.

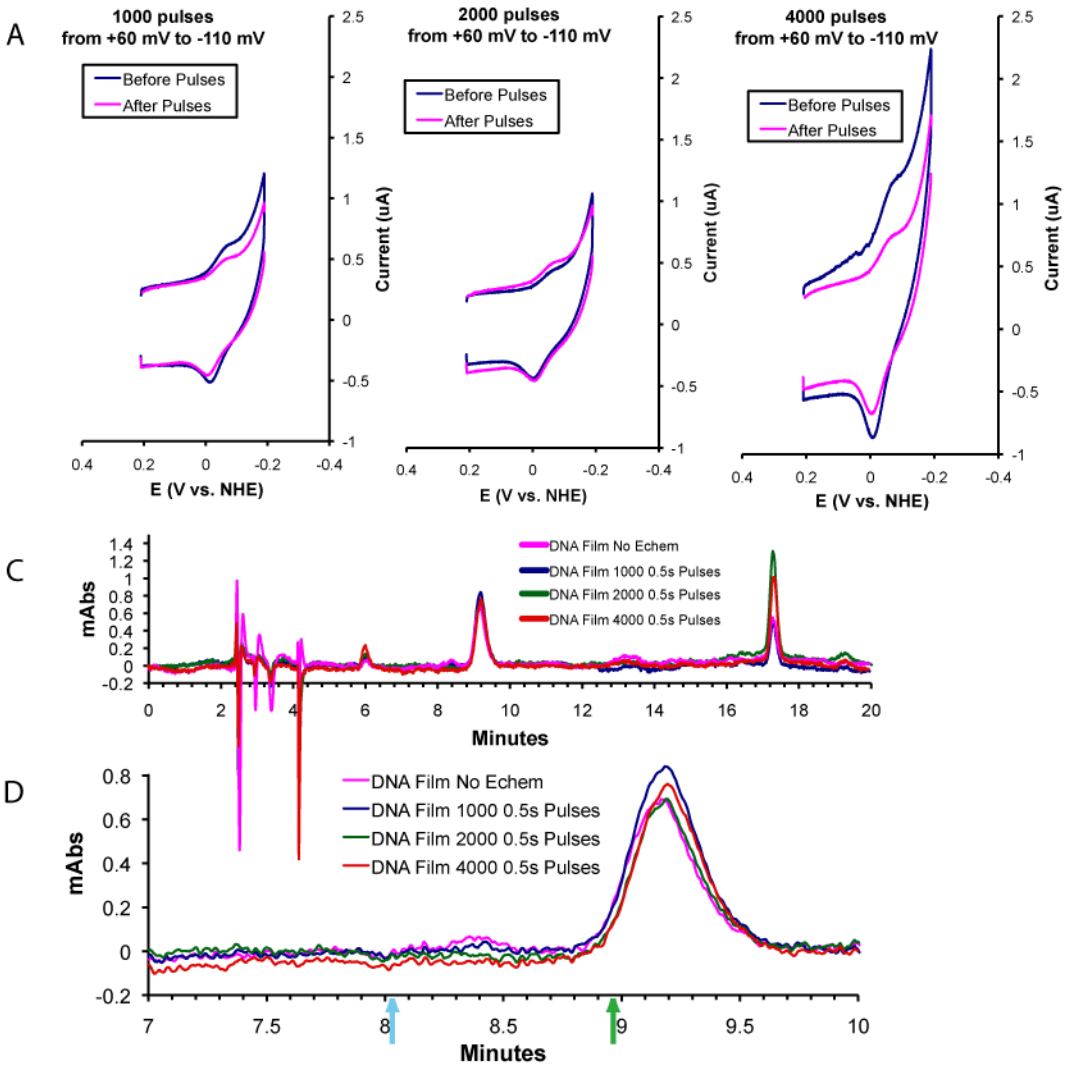

Figure 5.5. Analysis of ^{CP}C content after the pulse sequences *N* x (0.5 s, + 60 mV; 0.5 s, -110 mV). CV before and after the pulse sequences *N* x (0.5 s, + 60 mV; 0.5 s, -110 mV) (A), where *N* = 1000, 2000, 4000, show minimal effect of the pulse sequence on the film. No new peaks are observed in the DNA elution region of the HPLC chromatogram (260 nm) (C, D). The elution times of the standards for DNA with (green arrow) and without (cyan arrow) the ^{CP}C modification are indicated.

Table 5.1: Effect of pulse sequences on DNA monolayer coverage

Pulse Sequence	Quantification (in pmol/cm^2)		
	Before Pulses (by CV)	After Pulses (by CV)	Recovered (by stds)[a]
500 X 0.5 s, + 60 mV 0.5 s, -110 mV	27	27	n.d
1000 X 0.5 s, + 60 mV 0.5 s, -110 mV	10	8	12
2000 X 0.5 s, + 60 mV 0.5 s, -110 mV	11	10	10
4000 X 0.5 s, + 60 mV 0.5 s, -110 mV	23	14	11
1 X 1000 s, -110 mV	29	27	40
2 X 1000 s, -110 mV	10	6	8
4 X 1000 s, -110 mV	21	11	6
500 X 0.5 s, + 60 mV 0.5 s, -240 mV	10	11	10
1000 X 0.5 s, + 60 mV 0.5 s, -240 mV	16	15	30
2000 X 0.5 s, + 60 mV 0.5 s, -240 mV	16	11	10
500 X 0.5 s, + 60 mV 0.5 s, -340 mV	14	4	< 5
1000 X 0.5 s, + 60 mV 0.5 s, -340 mV	15	5	< 5
2000 X 0.5 s, + 60 mV 0.5 s, -340 mV	13	2	< 5

a) n.d. = not determined

Although previous work in our laboratory has found DNA films to be stable to electrochemical interrogation, the electrochemistry indicates that there is some superoxide generation at the electrode if the sample is not rigorously anaerobic, and hence it is not unreasonable to suspect that long pulse sequences might lead to some film degradation. The films were recovered and analyzed by HPLC. For each DNA film, substantial oligonucleotide is recovered, corresponding in elution to the ^{CP}C-containing strand. No evidence of the ring-opened product, or any other DNA, is observed.

Similar results were obtained for the pulse sequences N * (1000 s, -110 mV), where N = 1, 2, 4 (**Figure 5.6**), and for the pulse sequences N * (0.5 s, + 60 mV; 0.5 s, -240 mV) for N = 500, 1000, 2000 (**Figure 5.7**), although in the latter case, some degradation is observed for the longest pulse sequences. For the sequences N * (0.5 s, +60 mV; 0.5 s, -340 mV) for N = 500, 1000, 2000 (**Figure 5.8**), substantial degradation is observed (**Table 5.1**). As the cyclic voltammagrams and chronocoulometric traces both indicate substantial superoxide generation under these conditions, it is likely that the films themselves are decomposing. Strand cleavage should not be observable by our assay, as cleaved DNA would most likely be washed from the electrode during the initial washing steps of the recovery protocol. Nevertheless, the ring-opened product is not observed, despite detectable, though unquantifiable, levels of the intact deposited oligonucleotide being present.

There is a new peak under the most severe conditions (**Figures 5.7** and **5.8**), the UV-vis absorbance of which is consistent with it being an oligonucleotide, but the yield is too low for mass spectrometric analysis. Importantly, however, the height of this peak does not increase with increasing pulse number, indicating that it is not produced by electrochemistry; neither does the elution time correspond to that of the decomposition

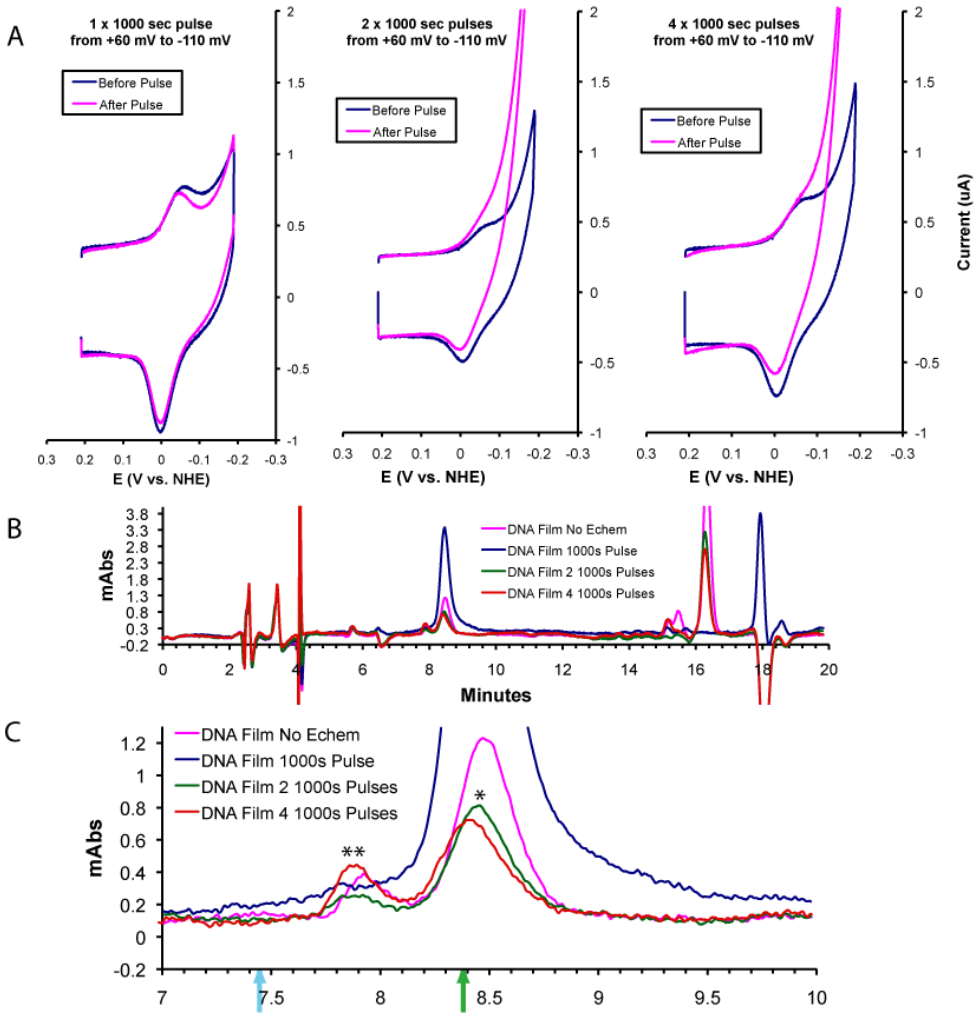

Figure 5.6. Analysis of ^{CP}C content after the pulse sequences *N* x (1000 s, -110 mV). CV before and after the pulse sequences *N* x (1000 s, -110 mV), where *N* = 1, 2, 4, show some effect of the pulse sequence on the film (A). The increase in background at high potentials is consistent with the generation of defects that allow increased access and consequent reduction of molecular oxygen. No new peaks emerge as a function of applied electrochemistry in the DNA elution region of the HPLC chromatogram (260 nm) (B, C). There is an uncharacterized peak (**), the area of which does not correlate with the applied electrochemistry, with UV-vis spectrum uncharacteristic of DNA, and present in the mercaptohexanol (no DNA) film. The elution times of the standards for DNA with (green arrow) and without (cyan arrow) the ^{CP}C modification are indicated.

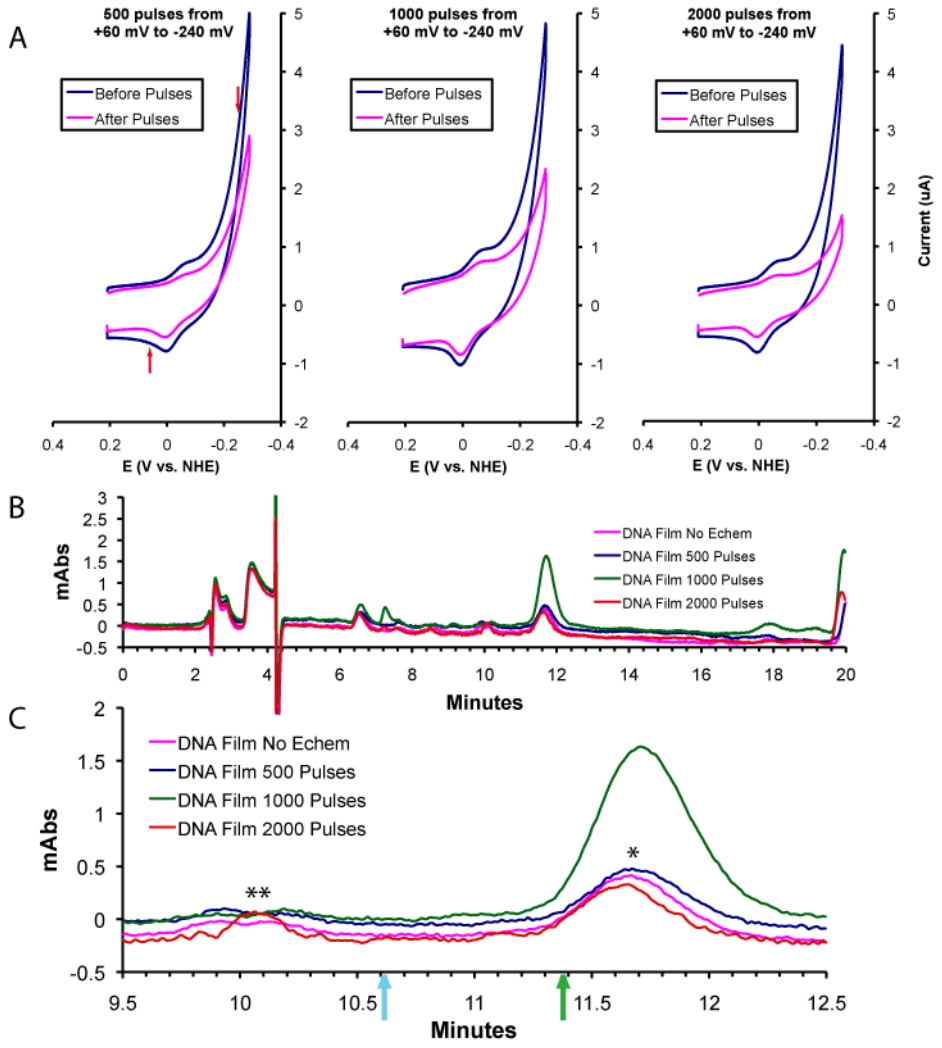

Figure 5.7. Analysis of ^{CP}C content after the pulse sequences *N* x (0.5 s, + 60 mV; 0.5 s, -240 mV). CV before and after the pulse sequences *N* x (0.5 s, + 60 mV; 0.5 s, -240 mV) (A), where *N* = 1000, 2000, 4000, show some effect of the pulse sequence on the film. The increase in background at high potentials is consistent with the generation of defects that allow increased access by and consequent reduction of molecular oxygen. No new peaks emerge as a function of applied electrochemistry in the DNA elution region of the HPLC chromatogram (260 nm) (B,C). There is an uncharacterized peak (**), the area of which does not correlate with the applied electrochemistry. The elution times of the standards for DNA with (green) and without (cyan) the ^{CP}C modification are indicated.

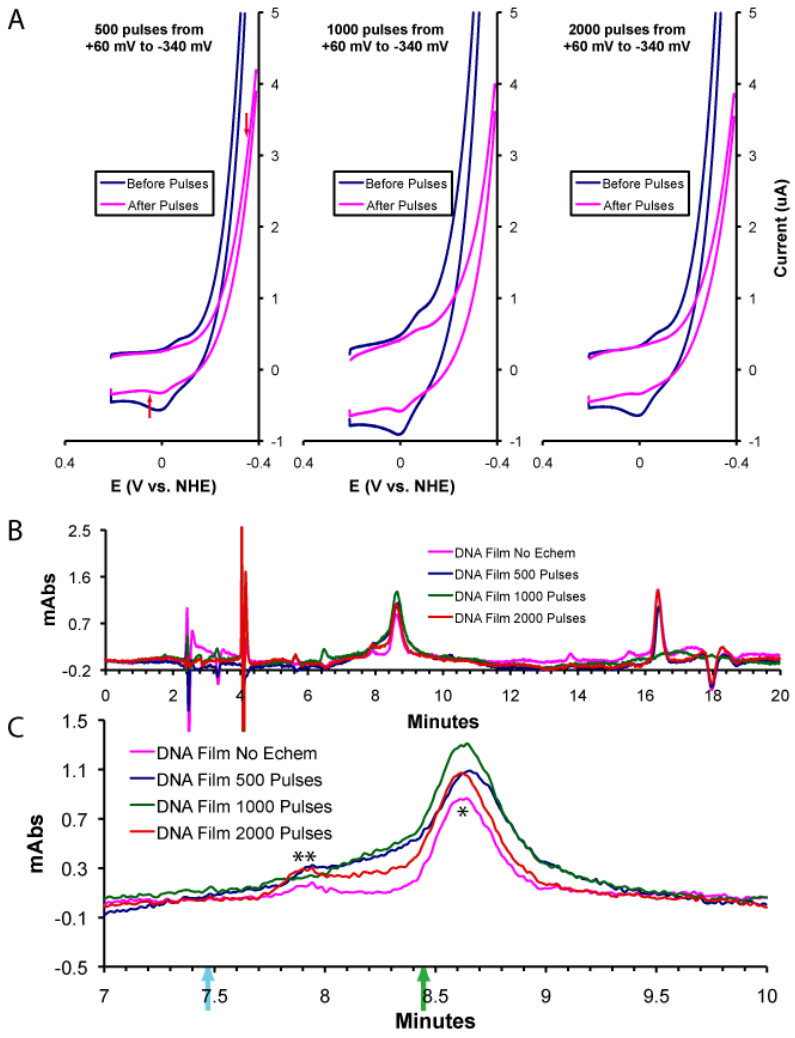

Figure 5.8. Analysis of ^{CP}C content after the pulse sequences *N* x (0.5 s, + 60 mV; 0.5 s, -340 mV). CV before and after the pulse sequences *N* x (0.5 s, + 60 mV; 0.5 s, -340 mV) (A), where *N* = 1000, 2000, 4000, show severe effect of the pulse sequence on the film. Besides the substantial increase in background, most of the faradaic signal associated with the Redmond Red is lost as the pulse sequence is extended. Although a new peak might emerge as a function of applied electrochemistry (**) in the DNA elution region of the HPLC chromatogram (260 nm) (B,C), it does not correspond to the decomposition standard. The elution times of the standards for DNA with (green) and without (cyan) the ^{CP}C modification are indicated.

standard. Hence, it is likely that this product corresponds to some other degradation process within the film, possibly due to superoxide reaction.

5.4. DISCUSSION

The electrochemistry, performed using the redox label Redmond Red with $E^{1/2}$ = -40 mV,[17] demonstrates the ability of DNA to mediate a charge at a potential far from the bases. How can we understand DNA-mediated electrochemistry that proceeds too far for superexchange, but at potentials incompatible with hopping? Decomposition of a radical trap on the bridge in response to DNA-mediated electrochemistry would demonstrate charge occupation of the bridge, and hence hopping as a mechanism for CT under these conditions. In contrast, superexchange involves only virtual occupation of the bridge, and hence would not lead to ^{CP}C decomposition. A lack of decomposition, as was observed here, is consistent with superexchange, and provides a strict limit on the time-scale of occupation if a hopping mechanism is in fact involved.

Consider the application of 4000 x (0.5 s, + 60 mV; 0.5 s, -240 mV) pulses (**Figure 5.7**). For low yields of decomposition:

$$Y = t_{EMF} f_{occ} k_{trap} \qquad (\mathbf{5.2})$$

where Y is the decomposition yield, t_{EMF} is the time of the applied potential, f_{occ} is the fraction of ^{CP}C occupied by the anion radical, and k_{trap} is the rate of trapping. Although k_{trap} has not been directly measured, we have demonstrated that it is greater than 1 x 10^9 s^{-1} for ^{CP}G;[25] we will use this value as a minimum. Our detection limit is certainly better than 5%. Hence, for the longest applied potential of 2000 total seconds, $f_{occ} < 2 \times 10^{-14}$. The presence of the redox probe is not a concern, since its potential is below the Fermi level and it is rapidly reduced. The reduced state will not compete for

transient occupation with the bridge. If transient states are indeed accessed, then they must satisfy the above constraint on f_{occ} since:

$$\int \frac{\phi(E)}{e^{(kT)^{-1}(E-E_{APP})}+1} dE = f_{occ} \qquad \textbf{(5.3)}$$

where $\phi(E)$ is the fraction of time that the LUMO of ^{CP}C has energy E and E_{APP} is -240 mV. For only two states, this corresponds to $\Delta G > 800$ mV, indicating that the equilibrium cytidine potential cannot be substantially above -1 V. The reduction potential of cytidine has been measured as about -2 V, so an equilibrium value far above that would have been surprising.

To evaluate the minimum potential for a transient state that is occupied on the time scale of DNA-mediated electrochemistry, we must know the coupling across the linker, which includes 14 methylenes. Then we can use the nonadiabatic CT relation:[28]

$$k_{CT} = \frac{k_B T\sqrt{\pi}}{\hbar\lambda} H_{DA}^2 \rho^{el} \int \frac{\exp\left\{-(E-\lambda+\eta)^2/(4\lambda k_B T)\right\}}{1+\exp(E/k_B T)} dE \qquad \textbf{(5.4)}$$

where H_{DA} is the donor-acceptor coupling, λ is the reorganization energy, ρ^{el} is the density of states on the electrode at the Fermi level,[29] and η is the overpotential, which is negative for endothermic injection. Over 14 methylenes, with $\beta \sim 1.1$ Å^{-1}, it would be surprising if the coupling is greater than 3×10^{-6} eV. Reorganization energies for CT in DNA have been estimated to range from 0.5 eV to 1 eV; for CT at an electrode the value will be approximately half, so here we will use the charitable value of 0.25 eV. If states on the DNA are in equilibrium, then

$$k_{obs} = f_{occ}\, k_{CT} \qquad \textbf{(5.5)}$$

This rate cannot satisfy the observed value of 30 s^{-1} for DNA-mediated electrochemistry,[8] subject to the constraint on f_{occ} determined above. For k_{CT} itself to be faster than 30 s^{-1},

the overpotential cannot be more than 120 mV above the potential of the probe. At that potential, the coupling between the DNA and the electrode must be at least 0.8 eV to both satisfy the constraint on DNA occupation and allow k_{obs} of 30 s^{-1}. Hence, hopping does not seem consistent with the present results.

On the other hand, these results are consistent with virtual occupation of the DNA bases, which does not lead to ring-opening. The challenge to this superexchange mechanism is the distance independence of the CT rate in DNA electrochemistry when the probe position is varied by 15 bases.[8] For a high energy barrier, the distance dependence of superexchange should be steep, but this is not experimentally observed. If low energy states are transiently formed to accommodate more facile superexchange, they will be subject to the same limitations of **Equation 5.3**. Furthermore, even for a low barrier where $V \sim \Delta\varepsilon$, the lower limit of β is about $0.7/a$ where a is the intersite distance on the bridge. For DNA base separation of 3.4 Å, and varying the probe position by 15 bases, this corresponds to a 3 x 10^5-fold drop in rate. For superexchange to be the mechanism of DNA-mediated electrochemistry, either the distance-dependence does not reflect a change in electronic coupling, or injection must be into a site fully delocalized on the DNA. The former case is true if the distance-dependence reflects conformational gating. This requires that CT be much faster than conformational gating even at long distances, and that the conformational gating occur faster than 30 s^{-1}. There are 14 methylenes in the linker between the DNA and the electrode. Taking β to be 0.2 $Å^{-1}$ in the DNA requires the rate through just the methylene linker to be 1 x 10^6 s^{-1}. To compare, the k^0 through 14 methylenes to ferrocene or pendant $[Ru(pyr)(NH3)_5]^{2+/3+}$ is about 1000 s^{-1}.[28] If we assume that 1000 s^{-1} is a reasonable value for oxidation of the probe at the first base, then for the rate over 15 bases to be below 30 s^{-1}, the β must be $\leq$ 0.07 $Å^{-1}$. This is

only reasonable if the sites that mediate superexchange are larger than a single base pair; for a low barrier, but still high enough to avoid hopping, the intersite distance must be at least three base pairs. Furthermore, if similar CT rates are observed over longer DNA bridges, the amount of delocalization that will be implied will be even greater. In summary, if superexchange is indeed the mechanism for DNA-mediated electrochemistry, there must be a transiently low barrier in the DNA, subject to the limits of **Equation 5.3**, and furthermore these states must be delocalized over several bases.

The above interpretation, however, is based on an absence of decomposition; if occupation does not lead to ^{CP}C decomposition in the monolayer, then **Equation 5.2** is not valid. It is possible that the environment around the ^{CP}C in films is not conducive to ring-opening, or that occupation at lower energy levels does not lead to trapping. A positive control would be necessary to demonstrate that we can perform ring-opening in films; current available modified bases are not within the electrochemical window of our system. This serves as an important caveat to the above analysis.

5.5 Conclusions

We have probed DNA-mediated electrochemistry in DNA-S/Au SAMs using a fast redox trap in the DNA bridge. To allow this measurement, we validated a protocol for oligonucleotide recovery analysis that allows us to observe and quantify the yield of chemical reactions in the monolayer. We do not observe any decomposition of the probe under conditions for which the monolayer is stable. If decomposition is an accurate proxy for cytidine occupation in monolayers, this result places a thermodynamic limitation on the energies and lifetimes of states that allow occupation of the DNA at applied potentials

far from the equilibrium potentials of the component nucleotides. It is hard to rationalize hopping with such a limit on DNA occupancy.

5.6. REFERENCES

(1) Jortner, J.; Bixon, M.; Langenbacher, T.; Michel-Beyerle, M.E. *Proc. Natl. Acad. Sci. U.S.A.* **1998**, *95*, 12759.

(2) Schuster, G. B., Ed. *Long-Range Charge Transfer in DNA, I and II;* Springer: New York, **2004**; Vols. 236, 237.

(3) Kelley, S.O.; Holmlin, R.E.; Stemp, E.D.A.; Barton, J. K. *J. Am. Chem. Soc.* **1997**, *199*, 9861.

(4) Murphy, C.J.; Arkin, M.R.; Jenkins, Y.; Ghatlia, N.D.; Bossmann, S.H.; Turro, N.J.; Barton, J.K. *Science* **1993**, *262*, 1025.

(5) Lewis, F.D.; Zhu, H.; Daublain, P.; Cohen, B.; Wasielewski, M.R. *Angew. Chem. Int. Ed.* **2006**, *45*, 7982.

(6) Treadway, C.R.; Hill, M.G.; Barton, J.K. *Chem. Phys.* **2002**, *281*, 409.

(7) Boal, A.K.; Genereux, J.C.; Sontz, P.A.; Gralnick, J.A.; Newman, D.K.; Barton, J.K. *Proc. Natl. Acad. Sci. U.S.A.* **2009**, *106*, 15237.

(8) Drummond, T.G.; Hill, M.G.; Barton, J.K. *Nat. Biotech.* **2003**, *21*, 1192.

(9) Inouye, M.; Ikeda, R.; Takase, M.; Tsuri, T.; Chiba, J. *Proc. Natl. Acad. Sci. U.S.A.* **2005**, *102*, 11606.

(10) Gorodetsky, A.A.; Green, O.; Yavin, E.; Barton, J.K. *Bioconjugate Chem.* **2007**, *18*, 1434.

(11) Kelley, S. O.; Jackson, N. M.; Hill, M. G.; Barton, J. K. *Angew. Chem., Int. Ed*. **1999**, *38*, 941.

(12) Boon, E. M.; Ceres, D. M.; Drummond, T. G.; Hill, M. G.; Barton J. K. *Nat. Biotech.* **2000**, *18*, 1096.

(13) Boal, A.K.; Barton, J.K. *Bioconjugate Chem.* **2005**, *16*, 312.

(14) Anne, A.; Demaille, C. *J. Am. Chem. Soc.* **2008**, *130*, 9822.

(15) Gorodetsky, A.A.; Buzzeo, M.C.; Barton, J.K. *Bioconjugate Chem.* **2008**, *19*, 2285.

(16) Steenken, S.; Telo, J.P.; Novais, H.M.; Candeias, L.P. *J. Am. Chem. Soc.* **1992**, *114*, 4701.

(17) Gorodetsky, A.A.; Dietrich, L.E.P.; Lee, P.E.; Demple, B.; Newman, D.K.; Barton, J.K. *Proc. Natl. Acad. Sci. U.S.A.* **2008**, *105*, 3684.

(18) Berlin, Y.A.; Grozema, F.C.; Siebbeles, L.D.A.; Ratner, M.A. *J. Phys. Chem. C* **2008**, *112*, 10988.

(19) Voityuk, A.A. *J. Chem. Phys.* **2008**, *128*, 115101.

(20) Elias, B.; Shao, F.; Barton, J. K. *J. Am. Chem. Soc.* **2008**, *130*, 1152.

(21) Elias, B.; Genereux, J.C.; Barton, J.K. *Angew. Chem. Int. Ed.* **2008**, *47*, 9067.

(22) Shao, F.; O'Neill, M. A.; Barton, J. K. *Proc. Natl. Acad. Sci. U.S.A.* **2004**, *101*, 17914.

(23) Shao, F.; Augustyn, K. E.; Barton, J. K. *J. Am. Chem. Soc.* **2005**, *127*, 17445.

(24) Murphy, J.N.; Chang, A.K.H.; Yu, H.-Z.; Bizzotto, D. *J. Am. Chem. Soc.* **2009**, *131*, 4042.

(25) Cf. footnote 22 in Chapter 2.

(26) Fiebig, T.; Wan, C.Z.; Zewail, A.H. *Chem. Phys. Chem.* **2002**, *3*, 781.

(27) Seidel, C.A.M.; Schulz, A.; Sauer, M.H.M. *J. Phys. Chem.* **1996**, *100*, 5541.

(28) Newton, M.D.; Smalley, J.F. *Phys. Chem. Chem. Phys.* **2007**, 9, 555.

(29) Traub, M.C.; Brunschwig, B.S.; Lewis, N.S. *J. Phys. Chem. B* **2007**, *111*, 6676.